ELSEVIER

Journal of Petroleum Science and Engineering 20 (1998) 283–296

JOURNAL OF PETROLEUM SCIENCE & ENGINEERING

Generalized adhesion maps for predicting thin film transitions

Aniello Mennella [a,*], Steven L. Bryant [b,1]

[a] *Eniricerche, 20097 S. Donato, Milanese, Italy*
[b] *TICAM, University of Texas at Austin, Austin, TX 78712, USA*

Accepted 21 January 1998

Abstract

Thin film transition (TFT) phenomena are of special interest to the petroleum industry. After crude-oil is trapped in reservoir rocks, it can alter the wettability of the rock surface, with profound implications for the subsequent transport of fluids. Correlation between the TFT and wettability alteration is qualitatively evident from many experiments. It is not clear, however, whether the TFT is a sufficient condition for wettability alteration. In this work we describe a generalized adhesion map, which locates the TFT in parameter space. Comparison of these maps with laboratory studies indicates that wettability alteration involves other mechanisms in addition to the TFT.

Keywords: reservoir wettability; crude-oil adsorption; adhesion; oil recovery

1. Introduction

A large body of evidence has accumulated in the past literature showing that oil reservoirs exhibit a broad spectrum of often complex wetting behaviors (Morrow, 1990). Because wettability is a key factor controlling both the distribution and displacement of immiscible phases in a porous medium, it is clear that recovery mechanisms, initial and residual fluid saturations and, therefore, overall reservoir performance may vary substantially between reservoirs, and even within a reservoir.

The availability of models able to predict the reservoir wettability state and its effect on the distribution of the reservoir fluids and the transport properties of the reservoir rock would eliminate a significant source of uncertainty in predicting reservoir performance. To this end, much research has addressed the following questions:

- What are the physical/chemical mechanisms that determine the wettability state in the reservoir?
- How do fluid transport properties depend on a given wettability state?

* Corresponding author. Fax: +39-2-52056364; e-mail: mennella@eniricerche.eni.it.
[1] Fax: +1-512-471-8694; e-mail: sbryant@ticam.utexas.edu.

0920-4105/98/$19.00
PII S0920-4105(98)00032-1

As to the first issue, many experimental studies have led to the definition of four main categories of crude-oil/brine/rock interactions, i.e., polar interactions, surface precipitation, acid/base and ion binding interactions (Buckley and Liu, 1996). Acid/base interactions, in particular, control brine film stability in presence of irreducible water saturation and can be described in terms of DLVO theory (Hirasaki, 1991). For certain values of the physical parameters (pH, salinity, applied capillary pressure), the film is stable only for molecular thicknesses; the transition that may occur from a thick to a thin film when some of the parameters are varied is called Thin Film Transition (TFT), and is generally believed to be a sufficient condition for subsequent adsorption of crude-oil components onto the solid surface (Kovscek et al., 1993).

This paper focuses on the application of the DLVO theory to prediction of TFT's and on the comparison of these predictions with literature adhesion tests experimental data. The theoretical approach is, as far as possible, general, that is to say, independent of the particular physical system considered. Following this approach, the concept of generalized adhesion map is introduced and applied to prediction of film stability boundaries in an adimensional parameter space. By comparing theoretical predictions with experimental observations, we highlight the limits of applicability of the DLVO approach and propose some hypotheses that may help in explaining the observed discrepancies.

2. Mathematical development

2.1. Interaction between two plane surfaces

The schematic in Fig. 1 shows two interfaces interacting through a liquid film. At large separation distances, the total force between the interfaces can be calculated from the DLVO theory. When the separation distance becomes small (< 1 nm) non-DLVO forces (e.g., structural and hydration forces) can play an important role and must therefore be taken into account. As our purpose is to determine the conditions for the stability of thick brine films, we neglect, as a first approximation, the contribution of short-range non-DLVO forces. Hydrophobic forces (that are long-range non-DLVO forces) are neglected in the following treatment; their role is discussed in Section 3.

2.1.1. Double layer interaction: the Poisson–Boltzmann equation

The interaction between charged surfaces in an electrolyte solution can be determined from the solution of the Poisson–Boltzmann equation, that describes the behavior of the potential between the interacting surfaces at

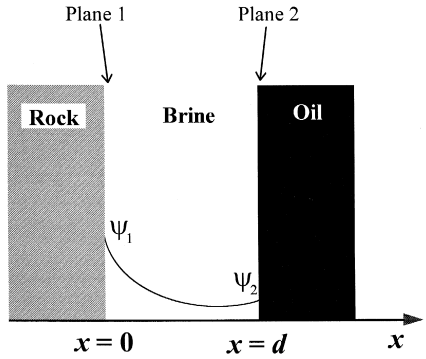

Fig. 1. Schematic of two plane surfaces (e.g., rock/brine and brine/oil interfaces) interacting through a liquid film (e.g., brine) of thickness d. Ψ_1 and Ψ_2 represent the value of the potential at the two interfaces. The behavior of the potential $\Psi(x)$ between the two interfaces can be determined from the solution of the non-linear Poisson–Boltzmann equation, Eq. (1).

a given separation distance. In the case of the one-dimensional system sketched in Fig. 1 for a symmetric electrolyte (e.g., NaCl), the equation, in normalized variables, takes the form (symbols and adimensional variables are defined in Section 5):

$$\frac{d^2 y}{d\xi^2} = \sinh(y). \tag{1}$$

The function $y(\xi)$ can be determined analytically from Eq. (1) and has different forms depending on the boundary conditions. A comprehensive table of such solutions can be found in McCormack et al. (1995).

In order to solve the Poisson–Boltzmann equation, either the surface potentials or the surface charges must be known. For plates at infinite distance, it is possible to infer the values of the surface potentials from (for example) zeta potential measurements, but at finite values of δ, it is necessary to make assumptions on their behavior vs. the distance of separation, δ. These relationships are usually called 'boundary conditions'.

A commonly used approach is the so-called 'constant potential boundary conditions' approximation, that assumes that the surface potentials remain constant at each value of δ. A more realistic approach is to consider that both the surface potentials and the surface charges can vary with the separation distance ('charge-regulating boundary conditions'). In this case, an additional relationship between surface potential and surface charge is needed, and it is usually obtained from the thermodynamics of the ion-exchange between the surface and the electrolyte solution (Takamura and Chow, 1985; Buckley et al., 1989).

Once the proper boundary conditions are fixed, it is possible to calculate the electrostatic component of the interaction, Π_{el}, that is dependent only on $y_{1\infty}$ and $y_{2\infty}$, i.e., the values of the surface potentials on the two planes when $\delta \to \infty$.

2.1.2. Van-der-Waals interaction

The second component considered is the van-der-Waals (vdW) interaction, that arises from the unbalance, across the interfaces, of molecular forces (dipole–dipole, dipole-induced dipole and dispersion forces). In the simplest approximation, the force per unit area is:

$$P_{vdW}(d) = -\frac{A}{6\pi d^3} \tag{2}$$

that can be written in a dimensional form as:

$$\Pi_{vdW}(\Omega, \delta) = -\frac{\Omega}{\delta^3} \tag{3}$$

The parameter $\Omega = \frac{A\kappa^3}{12\pi n_b kT}$ represents the ratio between the vdW and the electrostatic forces. An increase (decrease) in the parameter Ω corresponds to:

(i) an increase (decrease) in the Hamaker constant, A, or

(ii) an increase (decrease) of brine salinity (that determines a compression (expansion) of the double layer and, consequently, an increase (decrease) of the relative magnitude of vdW forces).

The total force per unit area, the disjoining pressure, can thus be written, in adimensional variables, as:

$$\Pi(y_{1\infty}, y_{2\infty}, \Omega, \delta) = \Pi_{vdW}(\Omega, \delta) + \Pi_{el}(y_{1\infty}, y_{2\infty}, \delta). \tag{4}$$

A unique disjoining pressure isotherm is hence determined once the surface potentials, the ratio vdW/double-layer (Ω), and the boundary conditions are defined.

2.2. Criteria for thin film transition

In Fig. 2, a calculated disjoining pressure isotherm is shown (parameters are indicated in the figure caption).

The presence of a maximum in the curve, Π_{crit}, implies that only for a limited range of values of the applied capillary pressure, Π_{appl}, the brine film may exist as a bulk liquid film. In fact, if Π_{appl} is greater than Π_{crit}, the film is unstable and collapses to molecular thicknesses (thin-film transition) at which it is stabilized by short-range forces.

For each boundary condition, the existence and the value of the maximum in the disjoining pressure isotherm is dependent on the particular choice of the parameters $y_{1\infty}$, $y_{2\infty}$ and Ω.

- In particular regions of the parameter space (for large values of Ω and/or when the potentials are of opposite signs) the maximum can be negative or even non-existent, so that the disjoining pressure isotherm is always negative and the force between the interfaces is attractive at all values of the separation distance. Existence of a bulk liquid film is therefore not possible for such parameter values.
- In other cases (for example when Ω is small and $y_{1\infty}$, $y_{2\infty}$ are large and of the same sign), the maximum is located at very small values of the separation distance ($\delta \ll 1$) where the repulsive structural forces become dominant. In this case, as the disjoining pressure isotherm is always positive, the brine film can exist as a bulk liquid film for a wide range of capillary pressure values.

As the function $\Pi_{crit}(y_{1\infty}, y_{2\infty}, \Omega)$ depends only on the particular choice for the boundary conditions, it can be used to predict the behavior of any given system for which the boundary conditions apply. Because thin-film transition phenomena are generally supposed to be correlated with wettability alteration phenomena (i.e., adhesion of crude-oil onto the solid), we denote the function $\Pi_{crit}(y_{1\infty}, y_{2\infty}, \Omega)$ with the term 'generalized adhesion map'.

2.3. Generalized adhesion maps

As previously defined, the generalized adhesion map is a three-dimensional hyper-surface embedded in a four-dimensional space. It is possible to reduce its dimensionality by fixing a certain value for the applied capillary pressure P_{appl}; the intersection of the plane $\Pi_{appl} = P_{appl}/2n_b kT$ with the surface $\Pi_{crit}(y_{1\infty}, y_{2\infty}, \Omega)$

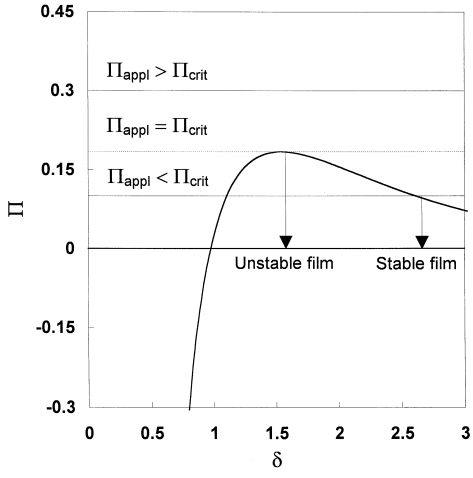

Fig. 2. Example of disjoining pressure isotherm displaying a maximum, Π_{crit}. If the applied capillary pressure, Π_{appl}, is less than Π_{crit} a stable 'thick' brine film exists. Otherwise, the film is unstable and collapses to molecular thicknesses. This particular example was calculated for the following parameter values: $y_{1\infty} = 1$, $y_{2\infty} = 1$, $\Omega = 0.038$, with constant potential boundary conditions.

determines a two-dimensional surface in the $\{y_{1\infty}, y_{2\infty}, \Omega\}$ space that represents the boundary between stable films (points below the surface) and unstable films (points above the surface). An example, calculated for $\Pi_{appl} = 0$ and constant potential boundary conditions, is shown in Fig. 3.

In order to check the dependency of the generalized adhesion maps on the boundary conditions, four generalized adhesion maps have been calculated for the following cases, i.e.:

1. both surfaces at constant potential (indicated with $\{p,p\}$),
2. both surfaces at constant charge (indicated with $\{c,c\}$),
3. one surface at constant charge and the other at constant potential (indicated with $\{p,c\}$), and
4. charge-regulating boundary conditions (indicated with {chr}).

It is worth noting that the map obtained using {chr} boundary conditions is not independent of the particular system considered, unlike the maps calculated with $\{p,p\}$, $\{c,c\}$ and $\{p,c\}$ boundary conditions. In fact, the charge-regulation model depends on the surface/brine ion exchange thermodynamics, that can vary, in principle, from system to system. In this particular case, we used a model that was derived for the Moutray-oil/brine/silica system, as detailed in Appendix A.

The results in Fig. 4 show that the maps relative to the $\{p,p\}$, $\{c,c\}$, and $\{p,c\}$ boundary conditions are very similar, especially in the parameter range $[y_{1\infty} < 2,\ y_{2\infty} < 2,\ \Omega < 4]$. Parameters relative to crude-oil/brine/solid systems are usually in the range $2 \le \text{pH} \le 10,\ 0.01 \le [\text{Na}^+] \le 1,\ 10^{-21} \le A \le 5 \times 10^{-19}$, that correspond to values of Ω in the range $0.03 \le \Omega \le 4$; this implies that these three possible choices for the boundary conditions are practically equivalent as far as the prediction of film stability is concerned.

The map obtained with charge-regulating boundary conditions (see Fig. 4d) looks, at first glance, very different from those depicted in Fig. 4a,b,c. If Ω is small ($\Omega < 1$), however, the error that is made by performing the calculation with the simplified boundary conditions is less than 10%.

The insensitivity of the generalized adhesion maps to the boundary conditions, however, can be observed only for low values of the applied capillary pressure (up to few tenths of KPa); when P_{appl} is high, the

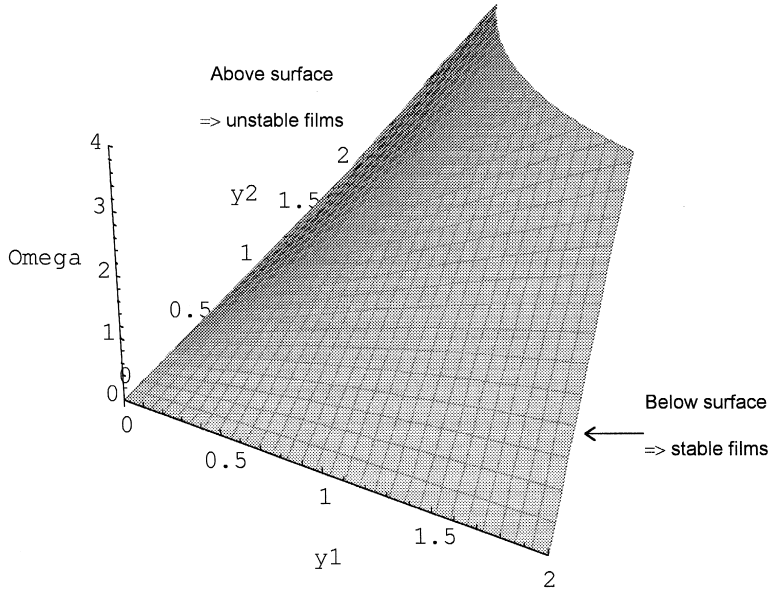

Fig. 3. Two-dimensional section of a generalized adhesion map calculated for constant potential boundary conditions. The section was determined for $\Pi_{appl} = 0$. Points below the surface are relative to parameters associated to stable bulk liquid films and vice versa.

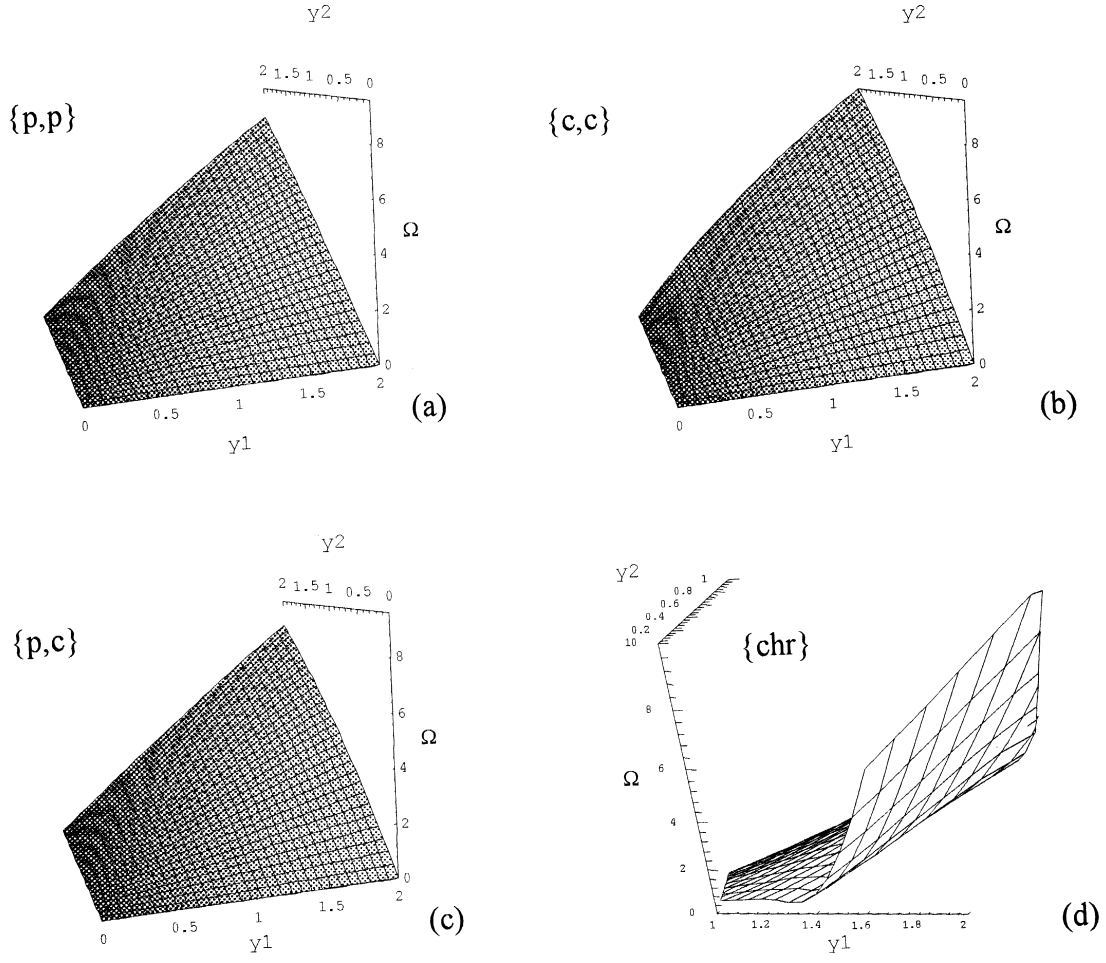

Fig. 4. Generalized adhesion maps determined for $\Pi_{appl} = 0$ and different choices for the boundary conditions. (a) Constant potential boundary conditions, $\{p, p\}$, (b) constant charge boundary conditions, $\{c, c\}$, (c) mixed boundary conditions (one surface at constant potential and the other at constant charge), $\{p, c\}$, and (d) charge-regulating boundary conditions, {chr}.

calculated map is generally dependent on the boundary conditions used to perform the calculation (Mennella and Bryant, 1996).

3. Examples of interpretation of laboratory data

3.1. Application of the generalized adhesion maps to adhesion test experimental data

Adhesion tests have often been used to assess the wetting properties of crude-oils on silica surfaces (Buckley et al., 1989, 1996). In the experiment, a captive drop of crude-oil is brought in proximity to a brine-covered glass slide. In these experiments, brines normally contain only a monovalent electrolyte (very often NaCl) to

avoid the occurrence of more complicated wetting phenomena induced by the presence of multivalent ions (ion-binding).

After some time (of the order of minutes) the drop is retracted and two behaviors are mainly observed:

- The drop retracts completely, leaving a clean surface (non-adhesion).
- The drop breaks during retraction, leaving some oil adhering to the surface (adhesion).

Temporary adhesion is also occasionally observed.

The physical parameters that are usually varied during the experiment are the brine pH and salinity; a {pH, Salinity} map that shows where adhesion and non-adhesion occur is generally called 'adhesion map'.

The {pH, Salinity} plane can be transformed in the adimensional coordinate system $\{y_1, y_2, \Omega\}$ provided that one knows the relationships between {pH, Salinity} and the surface potentials. In Fig. 5, an example of such a transformation is shown, where the zeta potential curves relative to the Moutray-oil/brine/glass system (Buckley et al., 1989) were used to perform the transformation. Fig. 5 also shows the intersection between the transformed plane and the generalized adhesion map calculated for $\Pi_{\text{appl}} = 0$ and $\{p, p\}$ boundary conditions; the resulting line defines the predicted boundary between adhesion and non-adhesion. The reduction of dimensionality (from the 2D surface, the generalized adhesion map, to the 1D line) is determined by fixing the value of the Hamaker constant, A (10^{-20} J in the example).

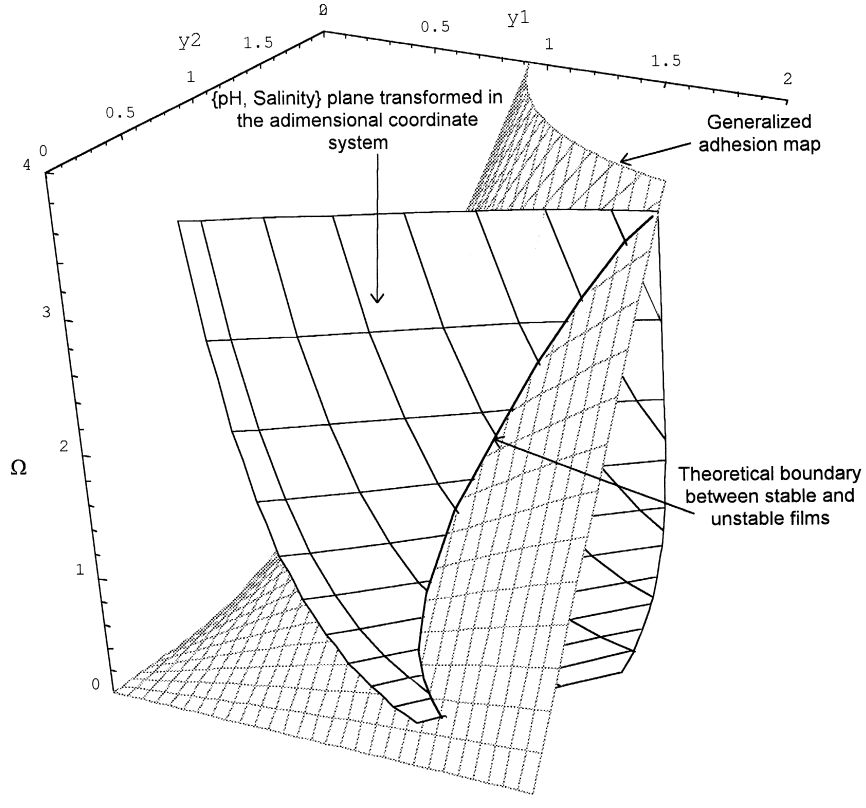

Fig. 5. The plane {pH, Salinity} transformed into the adimensional coordinate system intersects the generalized adhesion map calculated for constant potential boundary conditions. The intersection defines the theoretical boundary between stable and unstable films. Moutray-crude-oil/brine and silica/brine zeta potential curves were used to perform the transformation. The Hamaker constant was set to 10^{-20} J.

3.2. Comparison of predicted and observed adhesion boundary

An example that shows the adhesion behavior of Moutray-crude-oil on glass slides is represented in Fig. 6. Adhesion boundaries have been calculated using DLVO theory with both $\{p,p\}$ and {chr} boundary conditions, with the hypothesis $P_{appl} = 0$.

An additional calculated curve, taken from Buckley et al. (1989), is also shown in the Figure. In their calculations, performed with $\{p,p\}$ boundary conditions, they approximated the surface potential with the zeta potential; although this approximation does not influence predictions at low salinities, it changes dramatically the boundary shape when $[Na^+] > 0.1$ M, that diverges for concentrations greater than 0.2 M.

In the following, we will compare predicted boundaries with the experimental data and discuss the major discrepancies between theory and experiments.

3.2.1. Behavior at low salinities ($[Na^+] < 0.1$ M)

The observed boundary at low values of the salinity is approximately a horizontal straight line located at pH ≈ 6.5. DLVO theory predicts a qualitative similar behavior, independent of the boundary condition chosen, but with a quantitative mismatch of about 2.5 pH units.

Such mismatch can be explained invoking surface roughness as a means of increasing locally the applied capillary pressure. The capillary pressure necessary to shift the calculated boundary by 2.5 pH units ranges from 0.2 MPa (for $\{p,p\}$ boundary conditions) to about 2 MPa (for {chr} boundary conditions).

3.2.2. Behavior at high salinities ($[Na^+] \geq 0.1$ M)

As shown in Fig. 6, a second boundary between adhesion and non-adhesion is evident at a pH value of about 12. This second boundary cannot be predicted by the DLVO theory when the zeta potential curves are monotonic. However, experimental evidence exists for the reduction of zeta potential at high pH (Doe, 1994) which can explain the existence of a second boundary.

Although the data in Fig. 6 can be predicted by taking into account the above mentioned effects (surface roughness and reduction in zeta potential at high pH), many measurements of surface forces (Sharma, 1996) and adhesion tests reported by Buckley et al. (1996) have revealed another important qualitative discrepancy (not apparent from the data in Fig. 6), which is schematically represented in Fig. 7. In these experiments, non-adhesion behavior was observed when the salinity was increased, which determined the concave-down shape of the adhesion/non-adhesion boundary. This cannot be predicted by the DLVO approach used so far,

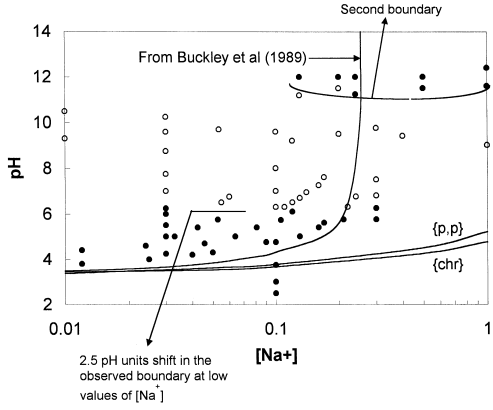

Fig. 6. Comparison of the adhesion boundary predicted from DLVO theory with adhesion test experimental data relative to Moutray-crude-oil/brine/glass system. Data are from Buckley et al. (1989). Theoretical boundaries have been calculated for $\{p,p\}$ and {chr} boundary conditions.

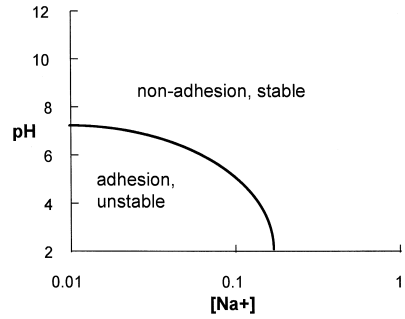

Fig. 7. Qualitative behavior of the adhesion boundary observed in a variety of experiments (Sharma, 1996; Buckley et al., 1996).

because in the DLVO theory an increase in salinity determines a compression in the double layer and a reduction in the magnitude of surface potentials, which both result in a decrease of the brine film stability.

In order to find possible explanations to this observed behavior, it is possible to formulate the following, mutually exclusive, hypotheses:

(i) in some regions of the parameter space the brine film remains thick even though the standard DLVO approach predicts its collapse, or

(ii) DLVO theory correctly predicts the qualitative behavior of thin film transition, but this does not provide a sufficient condition for wettability alteration when the salinity is high.

3.3. Extensions of the DLVO theory

We will firstly consider hypothesis (i) and check whether this could be verified by extending the standard DLVO approach with additional mechanisms.

3.3.1. Limits of the Poisson–Boltzmann equation

A basic assumption in the development of the Poisson–Boltzmann equation is that the average concentration of ions at a distance x from a charged interface is proportional to the potential in the same point (Verwey and Overbeek, 1948). This approximation is equivalent to assuming 'linearity' and 'additivity' of the potentials determined by all the surrounding ions and implies that the equation is strictly applicable when potentials and ion concentrations are low.

Although these limits have been recognized and discussed well before the development of the DLVO theory (Onsager, 1933), the Poisson–Boltzmann approach has often been used outside its strict domain of validity, mainly to avoid the much greater mathematical difficulties that would be encountered when attempting a more general approach. On the other hand, this approach has been often demonstrated to be robust also at extreme conditions (Israelachvili, 1991), and this has justified its use in a wide range of conditions.

These considerations, though not conclusive, lead us to doubt that the observed behavior could be explained in terms of a dramatic breakdown of the Poisson–Boltzmann approach at high salinity.

3.3.2. Effect of a stern layer

The assumption made in the standard DLVO theory that two interfaces can approach each other indefinitely can be corrected in order to take into account the finite size of transiently bound counterions (Frens and Overbeek, 1972). This is done by shifting the origin of the diffuse double layer at a finite distance, x_s—the Stern layer thickness—from the interface and assuming a linear decay of the potential across the layer. Even though this has a quantitative effect on the predicted boundary location (see Fig. 8), it is rather small and does not change the qualitative shape of the curve.

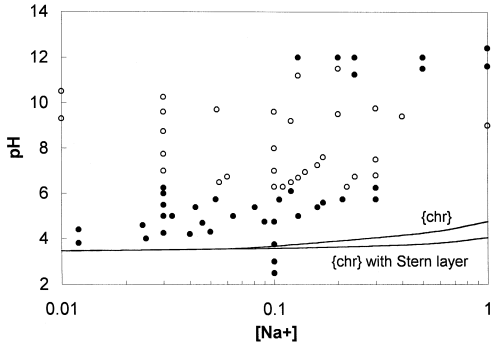

Fig. 8. Comparison of adhesion test data with adhesion boundary predicted from DLVO theory extended to include the presence of ions in the Inner Helmholtz Plane (Stern layer). Calculations have been performed using {chr} boundary conditions and a value of 0.2 nm for the thickness of the Stern layer.

3.3.3. Hydrophobic forces

Hydrophobic forces, often observed in systems that contain hydrophobic phases, are known to be long-range attractive forces, the origin of which has puzzled colloidalists for many years (Ninham, 1996). Recent research results indicate that long-range attractive forces can be determined by a variety of mechanisms depending on the particular system considered; a commonly observed behavior is the reduction of hydrophobic attraction with increasing salinity.

Even though the presence of hydrophobic forces in crude-oil/brine/solid systems cannot be ruled out completely, it is unlikely that they play a significant role in determining the trend shown in Fig. 7. In fact, even though the increase in salinity improves the film stability in systems that display hydrophobic attraction, this cannot exceed what is predicted by the simple DLVO approach that describes the behavior when hydrophobic forces are absent.

3.3.4. Dependency of vdW attraction on the electrolyte concentration

It is known that an increase in the electrolyte concentration determines a reduction of the vdW attraction (Israelachvili, 1991); this could therefore be a possible explanation for the observed behavior sketched in Fig. 7. In order to check this hypothesis, we have considered the following approximate form of the Hamaker constant (Israelachvili, 1991):

$$A = A_{v=0} + A_{v>0}. \tag{5}$$

In Eq. (5), A_{v0} represents the zero frequency term that is determined by permanent and induced dipoles, while $A_{v>0}$, the high-frequency term, accounts for dispersion forces.

As in the presence of an electrolyte, the zero-frequency term is screened by counterions, its contribution becomes negligible for separation distances greater than one half of the Debye length (Israelachvili, 1991). We can therefore consider only the dispersion term, that is dependent on the refractive indices of the interacting media, as shown in Eq. (6):

$$A_{v>0} = \frac{3h\nu_e \left(n^2_{\text{glass}} - n^2_{\text{brine}}\right)\left(n^2_{\text{oil}} - n^2_{\text{brine}}\right)}{8\sqrt{2}\left(n^2_{\text{glass}} + n^2_{\text{brine}}\right)^{1/2}\left(n^2_{\text{oil}} + n^2_{\text{brine}}\right)^{1/2}\left[\left(n^2_{\text{glass}} + n^2_{\text{brine}}\right)^{1/2} + \left(n^2_{\text{oil}} + n^2_{\text{brine}}\right)^{1/2}\right]}. \tag{6}$$

By knowing the behavior vs. salinity of the brine refractive index, n_{brine}, the index of refraction of glass, n_{glass}, and fixing the value of A at 10^{-20} J for $[Na^+] = 0.01$ M, it is possible to estimate the variation of A over the range in salinity 0.01 M ÷ 1 M. This variation has been found to be less than 10% which is not enough to explain the non-adhesion behavior observed at high salinities.

3.4. Role of short-range interactions

If no mechanism based on the long-range stabilization of brine films at high salinities can be successfully invoked to explain the observed data, one possible conclusion is that TFT may not be a sufficient condition for adsorption of crude-oil components onto the solid when the salinity is high.

In this hypothesis, short-range interactions and adsorption properties of crude-oils components through thin brine films would be the key factors in determining the wetting properties of crude-oils in presence of high salinity brines.

4. Conclusions

Wettability alteration properties of crude-oils have often been correlated with brine film stability, determined by the interplay of electrostatic and van-der-Waals interactions.

Generalized adhesion maps, calculated using a standard DLVO approach, have been used to investigate the occurrence of TFT in the parameter space of experimental conditions (i.e., infinite separation potentials and material properties) and check its dependency on the boundary conditions assumed for the double layer interaction. In the range of parameters normally encountered in crude-oil/brine/solid systems, the latter dependency has been found to be weak. The same conclusion holds when a more sophisticated charge-regulating model is used. An implication of this is that the simplest boundary condition can usually be applied if the purpose is to determine qualitative trends and/or when the uncertainties in the experimental data are high.

The observed discrepancies between calculated boundaries and experimental data reveal that the standard DLVO approach cannot be used in the entire parameter space to predict wettability alteration of a solid surface from crude-oil components. Although our examination of extensions of the DLVO framework is not exhaustive, the consistent trend of these calculations leads us to doubt whether any extension of the theory can explain these discrepancies. The root of this dilemma seems to be the underlying assumption that a transition to a thin film between an approaching oil phase and a mineral surface is a sufficient condition for adhesion of the oil phase to the mineral. It appears likely that other mechanisms are involved in wettability alteration under certain conditions.

5. Nomenclature

A	Hamaker constant (Joule)
A	Acidic or amphoteric species
B	Basic species
C	Integration constant present in the solution of the Poisson–Boltzmann equation
e	Elementary charge (C)
d	Distance between the two interfaces (m)
H^+	Hydrogen ion
h	Planck constant (Joule)
K	Dissociation constant (mol/1)
k	Boltzmann constant (Joule/K)
n	Refractive index, dimensionless
n_b	Number density of counter-ions in bulk (m^{-3})
N	Number densities of chemical species at the interface (m^{-2})
P	Pressure (Pa)
s	$ez\sigma/\kappa\varepsilon kT$, normalized surface charge density, dimensionless

T	Absolute temperature (°K)
x	Distance from one interface (m)
y	$ez\Psi/kT$, normalized surface potential, dimensionless
z	Valency of electrolyte ions, dimensionless
δ	κd, normalized distance between the two interfaces, dimensionless
ε	Electrical permittivity ($C^2\ s^2/(m^3\ Kg)$)
κ^{-1}	$\sqrt{\varepsilon kT/2e^2z^2n_b}$ Debye length (m)
υ_c	Main electronic absorption frequency in the UV (s^{-1})
Π	$P/2n_bkT$, normalized pressure, dimensionless
σ	Surface charge density ($C\ m^{-2}$)
ξ	κx, normalized distance, dimensionless
Ψ	Surface potential (V)
Ω	$A\kappa^3/(12\pi n_bkT)$, ratio of vdW over electrostatic forces, dimensionless

Subscripts

ac	acidic
amph	amphoteric
appl	applied
bas	basic
brine	pertaining to brine
crit	critical
el	electrical
glass	pertaining to glass
o	at the interface
oil	pertaining to oil
s	Stern layer
vdW	van der Waals
1	pertaining to surface 1
2	pertaining to surface 2
$+, -$	equilibria involving positively and negatively charged forms of amphoteric species
∞	limit when $\delta \to \infty$

Superscripts

amph	amphoteric
zwit	zwitterionic

Acknowledgements

We would like to thank Jill Buckley of PRRC (Socorro, NM) for her comments and suggestions. Eniricerche supported this research and permitted its publication.

Appendix A

The Ionizable Surface Group (ISG) Model has been applied to the glass/brine and oil/brine interfaces to derive the charge-regulating model used in our calculations. Details of the ISG Model and of its applications can be found, for example, in Takamura and Chow (1985) and Buckley et al. (1989).

A.1. Crude-oil / brine interface

The zwitterionic nature of the crude-oil/brine interface can be described by:

$$\begin{aligned} &AH \leftrightarrow A^- + H^+ \\ &BH^+ \leftrightarrow B + H^+ \end{aligned} \tag{A.1}$$

where A^- and BH^+ represent the acidic and basic groups at the interface. The dissociation constants are defined by $K_{ac} = [A^-][H_s^+]/[AH]$ and $K_{bas} = [B][H_s^+]/[BH^+]$.

$[H_s^+]$, the hydrogen ion concentration in proximity of the surface, can be related to the bulk ion concentration, $[H_b^+]$, via the Boltzmann relationship:

$$[H_s^-] = [H_b^+]\exp(-y_o^{zwit}). \tag{A.2}$$

Starting from Eq. (A.1), the following relationship between the adimensional surface charge density, s_o^{zwit}, and surface potential, y_o^{zwit}, can be derived (Takamura and Chow, 1985):

$$s_o^{zwit} = \frac{ze^2}{\kappa\varepsilon kT} N_{ac}\left[\frac{N_{bas}/N_{ac}}{1+(K_{bas}/[H_b^+])e^{y_o^{zwit}}} - \frac{1}{1+([H_b^+]/K_{ac})e^{-y_o^{zwit}}}\right] \tag{A.3}$$

where N_{ac} and N_{bas} represent the number density of acidic and basic sites at the interface.

A.2. Glass / brine interface

The amphoteric nature of the glass/brine interface can be described by:

$$\begin{aligned} &AH_2^+ \leftrightarrow AH + H^+ \\ &AH \leftrightarrow A^- + H^+ \end{aligned} \tag{A.4}$$

with dissociation constants $K_+ = [AH][H_s^+]/[AH_2^+]$ and $K = [A^-][H_s^+]/[AH]$.

In a similar fashion, one can calculate the adimensional surface charge density as:

$$s_o^{amph} = \frac{ze^2}{\kappa\varepsilon kT} N_{amph} \frac{([H_b^+/K_+)e^{-y_o^{amph}} - ([K_-/[H_b^+])e^{y_o^{amph}}}{1+([H_b^+]/K_+)e^{-y_o^{amph}} + (K_-/[H_b^+])e^{y_o^{amph}}}. \tag{A.5}$$

In the calculation of the electrostatic component of the disjoining pressure isotherm, Eqs. (A.3) and (A.5) must be equated, at each value of the separation distance, δ, to the charge in the double layer given by:

$$\begin{aligned} s_o^{zwit} &= \pm\sqrt{2\cosh y_o^{zwit} + C(\delta)} \\ s_o^{amph} &= \pm\sqrt{2\cosh y_o^{amph} + C(\delta)} \end{aligned} \tag{A.6}$$

where $C(\delta)$ is determined by solving, for each value of δ, the Poisson–Boltzmann equation with the above boundary conditions.

Table 1
Material constants for Moutray-crude-oil/brine and glass/brine interfaces

Moutray-crude-oil			
$N_{ac} \times 10^{18}$	$N_{bas} \times 10^{18}$	pK_{ac}	pK_{bas}
0.5	0.1	4.0	7.0
Glass			
$N_{amph} \times 10^{18}$	–	pK_+	pK
2.5	–	−1.0	4.0

Physical parameters relative to Moutray-crude-oil/brine and glass/brine interfaces, necessary for the calculations, have been taken from Buckley et al. (1989) and are reported in Table 1.

References

Buckley, J.S., Liu, Y., 1996. Some mechanisms of crude-oil/brine/solid interactions. Presented at the 4th Int. Symp. on Evaluation of Reservoir Wettability and its Effect on Oil Recovery, Montpellier, France, Sept. 11–13, 1996.

Buckley, J.S., Takamura, K., Morrow, N.R., 1989. Influence of electrical surface charges on the wetting properties of crude-oils. Soc. Pet. Eng. Reservoir Eng. (Aug.), pp. 332–340.

Buckley, J.S., Liu, Y., Xie, X., Morrow, N.R., 1996. Asphaltenes and crude-oil wetting—the effect of oil composition. Presented at Soc. Pet. Eng. Improved Oil Recovery Symp., Tulsa, OK, April 21–23, 1996, SPE Pap. 35366.

Doe, P., 1994. Salinity dependence in the wetting of silica by oils. Presented at the 3rd Int. Symp. on Evaluation of Reservoir Wettability and Its Effect on Oil Recovery, Laramie, WY, Sept. 21–23, 1994.

Frens, G., Overbeek, J.Th.G., 1972. Repeptization and the theory of electrocratic colloids. J. Colloid Interface Sci. 38, 376–387.

Hirasaki, G.J., 1991. Wettability: fundamentals and surface forces. Soc. Pet. Eng. Formation Evaluation (June), pp. 217–226.

Israelachvili, J., 1991. Intermolecular and Surface Forces. Academic Press, New York.

Kovscek, A.R., Wong, H., Radke, C.J., 1993. A pore level scenario for the development of mixed wettability in oil reservoirs. AIChE J. 39 (6), 1072–1085.

McCormack, D., Carnie, S.L., Chan, D.Y.C., 1995. Calculations of electric double-layer force and interaction free energy between dissimilar surfaces. J. Colloid Interface Sci. 169, 177–196.

Mennella, A., Bryant, S.L., 1996. Existence and sensitivity of the wetting transition under various boundary conditions. Presented at the 11th Int. Conf. on Surface Forces, Moscow, Russia, June 25–29, 1996.

Morrow, N.R., 1990. Wettability and its effect on oil recovery. J. Pet. Technol. (Dec.), pp. 1476–1484.

Ninham, B.W., 1996. Water, oil, gas and electrolyte. Emerging ideas on the puzzle of hydrophobic interactions. Presented at the 11th Int. Conf. on Surface Forces, Moscow, Russia, June 25–29, 1996.

Onsager, L., 1933. Theories of concentrated electrolytes. Chem. Rev. 13, 73–89.

Sharma, M., 1996. Measurement of critical disjoining pressure for dewetting of solid surfaces. J. Colloid Interface Sci. 181, 443–455.

Takamura, K., Chow, R.S., 1985. The electric properties of the bitumen/water interface: Part II. Application of the ionizable surface group model. Colloids Surf. 15, 35–48.

Verwey, E.J.W., Overbeek, J.T.G., 1948. Theory of the Stability of Lyophobic Colloids. Elsevier, Amsterdam.